# Influence of Environmental Degradation on Dynamic Properties of Masonry Bridges

**Conference Paper** · June 2016



**3 authors:**

Andrea Benedetti
University of Bologna


John Nichols
Texas A&M University


Adrienn K Tomor
University of the West of England, Bristol

# Influence of Environmental Degradation on Dynamic Properties of Masonry Bridges

A. Benedetti
*University of Bologna, DICAM Department, 2 Viale Risorgimento, 40136 Bologna, Italy*

J. Nichols
*Texas A & M University, College of Architecture, 3137 TAMU, College Station, Texas, USA*

A. Tomor
*University of West of England, Department of Architecture and Built Environment, BS161QY, Bristol, U.K.*

ABSTRACT: The paper presents some preliminary analyses devoted to the identification of suitable models able to provide the frequency decay of a damaged masonry structure on the basis of the observed damage pattern. In particular the analysis will be carried out with reference to some comparison FE models, and by introducing two distinct damage patterns, i.e. an elastic modulus decay of an external layer of the bridge arch, or a localised reduction of section due to impact or brick and stone detachments. The worked out examples allow checking of a very simple formulation based on the frequency evaluation through the static displacement equivalence of energy, and the splitting of the curvature diagram in the average part plus an added impulse term due to the presence of defects. The proposed formula is in good agreement with the FE analyses and sufficiently simple to be used for the detection of the damaged material properties, as a function of the average frequency decay.

## 1 INTRODUCTION

The long term monitoring of bridges requires information about the signatures produced in the dynamic properties of the bridge by the deterioration factors acting on the bridge itself (Salawu 1997). While in general for concrete and steel bridges the most influential factors are localised damages produced by impacts or fatigue cracks, in masonry bridges a very important role is played by environmental degradation of mortar and blocks (Benedetti et Al. 2010).

Starting from previous studies dealing with the relationship between material properties decay and harsh environmental conditions such as marine spray or contaminated damp, some preliminary analyses are carried out in order to connect recorded variations in the dynamic properties of a bridge with a given level of damage suffered by the masonry material. Very important factors of the analysis are the influence of cracks in increasing the depth of the degraded layer, and the effect of repair works such as repointing of the mortar courses and substitution of the exfoliated bricks.

As a first step in the definition of a precise identification procedure, in this paper the analysis is carried out with reference to very idealised situations, such as the presence on the bottom face of the bridge of a continuous layer of damaged material, or the presence of a local intake caused by impact or local de-cohesion of the masonry texture. The comparison will be performed versus a series of 2-D Finite Element models, which will constitute the reference group in checking the effectiveness of the proposed formula (Doebling et Al. 1996).

The influence of the structural damage in terms of change of natural frequencies is dealt with by introducing in the static equivalence to the dynamic vibration formula, the effect of the damage as a change in the curvature diagram. As in the case of continuous deterioration, the change concerns the bridge section becoming a bi-modulus arch, where as in the case of a localised defect, the change is linked to a curvature spike (Gillich 2014).

Although the analysis is based on the study of a straight beam, it is fully applicable to circular arches, as pointed out by Öz and Daş (2006), simply by changing the abscissa with the curvilinear abscissa.

In the paper three arches with different opening angle are used as a data set by introducing six different damage patterns. The comparison of the numerical frequency decay with the one predicted by the developed formula shows a good agreement over the whole comparison data set.

The preliminary results of this work implemented as a step in the SHAPE research project granted by the INFRAVATION call, let us understand that the frequency decay deserves special attention as a warning parameter since some defects produce an uneven change on the frequency set of a bridge structure.

## 2 FREQUENCY OF A DAMAGED BEAM

As is well known, the natural frequency of a beam with distributed mass and eventually a concentrated mass over it, can be obtained through the equivalence of the kinetic energy of the vibration mode and the potential energy of one equivalent deflected shape of the beam under a concentrated force.

The concentrated force to be applied on the beam corresponds to a given fraction of the beam weight, depending on the position in which we want to concentrate the beam distributed mass (Belluzzi 1960). If the selected force position along the beam, divides the beam length $L$ in two parts $a$ and $b$, we obtain the weight fraction as:

$$\Delta P = G \cdot \frac{2 \cdot \left(a^5 + b^5\right) + 14ab \cdot \left(a^3 + b^3\right) + 35a^2b^2L}{105 \cdot a^2b^2L} \tag{1}$$

Where $G$ is the total beam weight. When the mid span is selected, the resulting fraction is $17/35 \cdot G$.

The natural frequency of the beam can be expressed as a function of the displacement occurring under this force. If we consider a simply supported beam, the displacement is:

$$\delta'(L/2) = \frac{17G}{35} \cdot \frac{L^3}{48 \cdot EJ} \tag{2}$$

Where $E$ and $J$ are the elastic modulus and the inertia moment of the beam section.

The natural frequency is finally obtained as:

$$f_0 = \frac{1}{2\pi} \cdot \sqrt{\frac{g}{\delta_{stat}}} \tag{3}$$

With $g$ the gravity constant 9,81 m/s$^2$ and the other frequencies can be computed with the square of the order number $n^2$.

If the beam has a damaged section, the displacement is increased by the concentrated curvature spike resulting from the local loss of rigidity, as in figure 1.

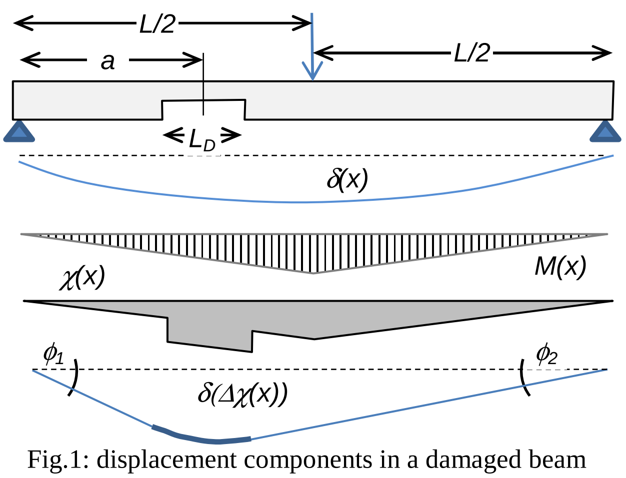

Fig.1: displacement components in a damaged beam

The decrease of natural frequency of a damaged beam is strictly related to the increase in displacement given by the curvature spike resulting from the loss of rigidity of the damaged section.

The displacement increase can be computed in a simplified and easy way, by considering a total rotation of the two beam arms as $\Delta\chi \cdot L_c$, and the continuity equation of the displacement:

$$\delta'' = \phi_1 \cdot a = \phi_2 \cdot (L - a) \tag{4}$$

$$\Delta\chi(a) = \frac{M(a)}{EJ_D} - \frac{M(a)}{EJ} = \chi(a) \cdot \left(\frac{EJ}{EJ_D} - 1\right) \tag{5}$$

Where $EJ$ is the rigidity of the undamaged section while $EJ_D$ is the one of the damaged part.

The increment of displacement in the mid span produced by the localized damage is:

$$\delta'' = \frac{17}{140} \cdot \frac{Ga^2L_D}{EJ} \cdot \left(\frac{EJ}{EJ_D} - 1\right) \tag{6}$$

And therefore the shift of frequency due to the localized damage holds:

$$f_{0,D} = f_0 \cdot \left[1 + 12\frac{a^2L_D}{L^3} \cdot \left(\frac{EJ}{EJ_D} - 1\right)\right]^{-1/2} \tag{7}$$

It is to point out that the formula is correct until the size of the damaged zone is small enough; if the damage is extended over the whole span of the structure the shift factor becomes:

$$f_{0,D} = f_0 \cdot \left[1 + \frac{L_D}{L} \cdot \left(\frac{EJ}{EJ_D} - 1\right)\right]^{-1/2} = f_0 \cdot k_D \tag{8}$$

That means that if $a$ is larger than 30% of $L$ approximately, the second formula should be used. In real application, unless the damaging factor is an impact against the bridge, the formula (8) can be used with an acceptable approximation.

In order to assess the efficiency of the proposed formulation, a parametric investigation is performed by using as reference set a series of Finite Element analyses of hinged-hinged arches.

## 3 EVALUATION OF THE DAMAGED AREA

The damaged section rigidity is easily calculated by inverting formula (8). In particular we obtain:

$$n = \frac{EJ_D}{EJ} = \left[1 + \left(\frac{1}{k_D^2} - 1\right)\frac{L}{L_D}\right]^{-1}, \tag{9}$$

And this allows evaluating the size of the damaged zone simply by using a bi-modulus section geometry.

If the damaged section has a layer of thickness $c$ of reduced elastic modulus $E_D$, we can express by well-known mass geometry formulas the section rigidity. By setting:

$$\rho = \frac{c}{h} \ , \ \mu = 1 - \frac{E_D}{E}, \tag{10}$$

it is possible to compute the ratio $n$ as a function of the parameters $\rho$ and $\mu$:

$$n = \frac{1 - 4\mu\rho + 6\mu\rho^2 - 4\mu\rho^3 - \mu^2\rho^4}{1 - \mu\rho}. \tag{11}$$

Since the value of $\rho$ is in general small, it is possible to approximate this value by the series expansion around 0 up to the second term.

$$n = 1 - 3\mu\rho + 3\mu^2\rho^2 \frac{(2-\mu)}{\mu}. \tag{12}$$

The following figure 2 represents the ratio of the approximated expansion (12) as a ratio of the exact formula (11). The fit is very good for the range of practical values of the observable damage.

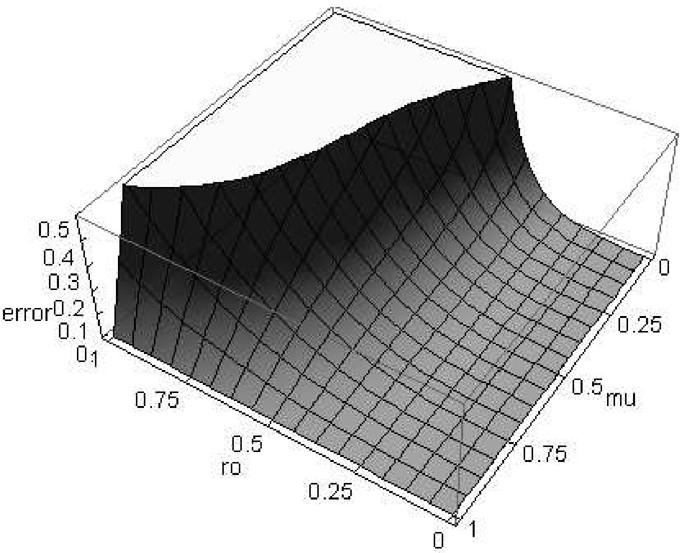


Figure 2. Error plot of the series expansion

Assuming that the last coefficient of Eq. (12) is in the range {1;3}, we can extract an approximate value of the product $\rho \cdot \mu$:

$$\mu\rho = \frac{\sqrt{5 - 4 \cdot n} - 1}{3}. \tag{13}$$

Once the elastic modulus decay is estimated by on site testing methods or assuming a sensible reduction factor ($\mu$ = 1 for missing material), the damaged thickness of the considered section is easily determined.

The given formula has been tested against the numerically simulated damage patterns described in the next section.

## 4 PARAMETRIC VERIFICATION

The verification of the proposed formula was performed with reference to a prototype arch of 4.4 m radius and section 0.8·1,0 $m^2$. The modulus is set as 6000 MPa and the mass density as 1800 $kg/m^3$. Three different arch openings are considered, namely 180°, 135° and 90° degrees.

The damaged material is assumed to suffer a reduction of 50% the modulus, and when a localized damage is present, the arch thickness is reduced of 0.1 or 0.2 m. As a concern, six different cases have been verified, as is shown in the following Figure 3 and Table 1.

The selected cases encompass three models in which a general damage is widespread over the lower face of the arch, as a simulated weathering condition in which mortar and bricks are degraded.

Other three models present localized zones of missing material at the crown and at the voussoir, as a consequence of a local defect or impact.

Table 1. Description of the examined cases.

| Case | Damage | Thickness [m] | Length [m] | Position [m] |
|---|---|---|---|---|
| A | reference | 0.10 | - | - |
| B | material | 0.10 | total | - |
| C | material | 0.20 | total | . |
| D | material | 0.10-0.20 | total | - |
| E | intake | 0.20 | 0.40 | voussoir |
| F | intake | 0.10 | 0.80 | center |
| G | intake | 0.20 | 1.20 | center |

The computed first ten frequencies of the three reference arches are reported in the following table 2.

Table 2. Frequencies of the reference arches.

| | Arch Opening | | |
|---|---|---|---|
| Frequency | 180° | 135° | 90° |
| 1 | 7.73 | 17.21 | 44.36 |
| 2 | 22.88 | 41.48 | 58.07 |
| 3 | 44.80 | 65.30 | 105.56 |
| 4 | 60.14 | 78.89 | 139.93 |
| 5 | 75.82 | 108.48 | 175.40 |
| 6 | 86.90 | 124.92 | 244.60 |
| 7 | 106.38 | 172.34 | 270.78 |
| 8 | 133.59 | 184.47 | 326.47 |
| 9 | 147.78 | 222.61 | 395.07 |
| 10 | 171.47 | 265.09 | 408.22 |

The following tables report the variation of the frequencies as a function of the seven examined damage patterns. It is important to note that localized damage gives rise to alternate increase and decrease of frequency values, while for the case of distributed damage, the frequency shift is evenly distributed in the frequency range and approximately linear with the damage level.

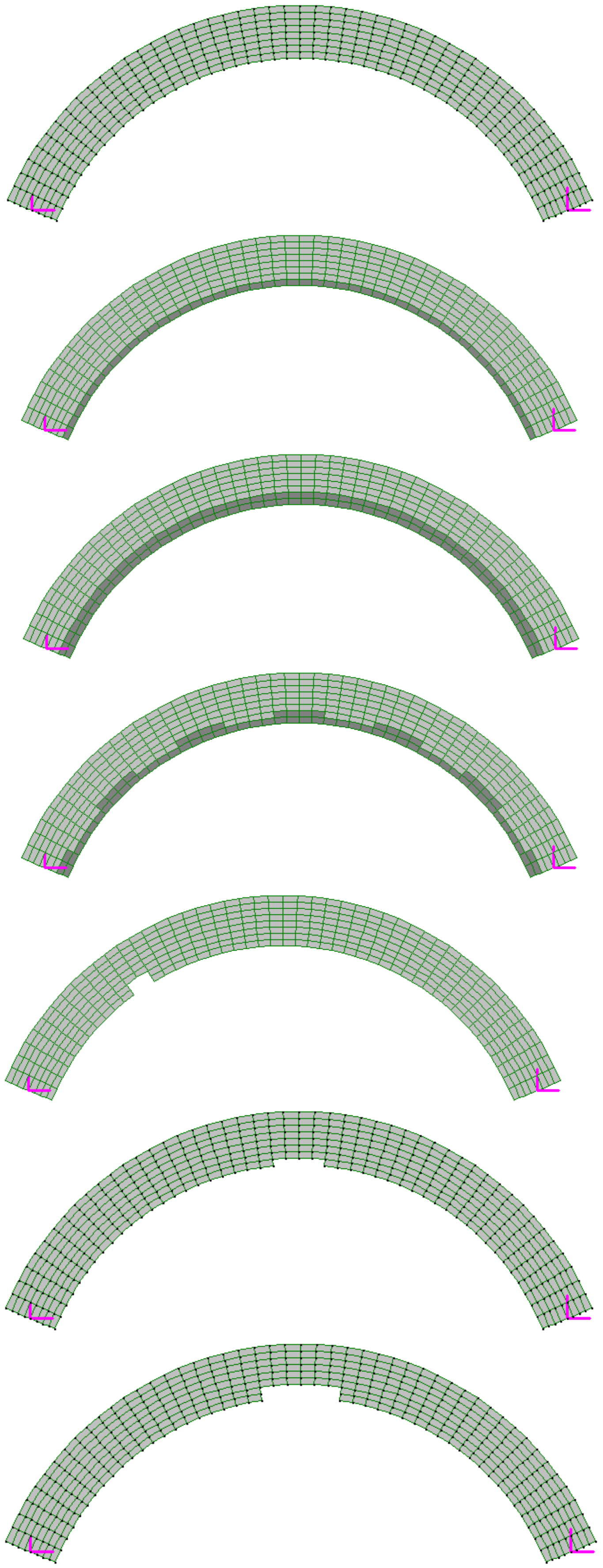

Fig. 3: The seven examined arch cases. The damaged material in dark grey.

The following tables list the main 10 frequencies of the 18 examined cases for the 6 damage patterns.

Table 3.a. Frequency fractions of the 180° arch.

| Case | B | C | D | E | F | G |
|---|---|---|---|---|---|---|
| Freq. | [%] | [%] | [%] | [%] | [%] | [%] |
| 1 | 90.9 | 85.1 | 87.8 | 93.4 | 100.4 | 100.7 |
| 2 | 90.9 | 84.9 | 87.6 | 96.9 | 98.0 | 94.1 |
| 3 | 91.2 | 85.3 | 88.0 | 100.1 | 99.9 | 98.1 |
| 4 | 94.9 | 90.1 | 92.2 | 100.9 | 97.0 | 91.3 |
| 5 | 93.9 | 89.8 | 91.7 | 95.8 | 100.0 | 101.3 |
| 6 | 95.5 | 91.0 | 93.0 | 100.6 | 100.3 | 99.8 |
| 7 | 94.1 | 90.4 | 92.2 | 94.7 | 99.7 | 97.4 |
| 8 | 92.7 | 87.4 | 89.7 | 98.4 | 96.8 | 92.8 |
| 9 | 97.2 | 94.4 | 95.8 | 99.9 | 100.5 | 101.2 |
| 10 | 92.8 | 87.7 | 88.9 | 99.3 | 99.5 | 95.7 |

Table 3.b. Frequency fractions of the 135° arch.

| Case | B | C | D | E | F | G |
|---|---|---|---|---|---|---|
| Freq. | [%] | [%] | [%] | [%] | [%] | [%] |
| 1 | 90.9 | 84.9 | 87.6 | 91.7 | 100.4 | 100.0 |
| 2 | 91.3 | 85.2 | 88.1 | 95.8 | 99.0 | 97.2 |
| 3 | 97.1 | 94.2 | 95.5 | 101.0 | 96.9 | 91.8 |
| 4 | 91.6 | 85.7 | 88.5 | 100.0 | 99.6 | 96.5 |
| 5 | 97.6 | 94.9 | 96.1 | 99.2 | 100.5 | 100.5 |
| 6 | 92.4 | 87.2 | 89.6 | 96.8 | 98.6 | 98.3 |
| 7 | 93.0 | 88.1 | 91.5 | 95.2 | 99.3 | 94.8 |
| 8 | 97.1 | 93.7 | 95.3 | 100.4 | 97.8 | 94.6 |
| 9 | 93.6 | 89.3 | 91.2 | 97.8 | 99.3 | 99.6 |
| 10 | 94.7 | 89.9 | 92.6 | 99.2 | 99.9 | 95.9 |

Table 3.c. Frequency fractions of the 90° arch.

| Case | B | C | D | E | F | G |
|---|---|---|---|---|---|---|
| Freq. | [%] | [%] | [%] | [%] | [%] | [%] |
| 1 | 91.0 | 84.9 | 87.7 | 88.8 | 100.2 | 97.3 |
| 2 | 96.9 | 93.4 | 95.1 | 98.8 | 101.8 | 104.7 |
| 3 | 93.2 | 88.7 | 90.7 | 98.2 | 94.6 | 88.9 |
| 4 | 96.0 | 91.6 | 94.1 | 99.9 | 100.3 | 100.6 |
| 5 | 94.5 | 91.0 | 93.3 | 98.5 | 99.3 | 93.1 |
| 6 | 93.0 | 87.9 | 90.5 | 96.7 | 99.3 | 98.5 |
| 7 | 97.8 | 95.1 | 95.8 | 100.5 | 97.5 | 95.2 |
| 8 | 93.7 | 89.0 | 90.9 | 95.6 | 98.3 | 93.5 |
| 9 | 97.3 | 92.8 | 94.9 | 98.4 | 100.4 | 99.4 |
| 10 | 94.5 | 91.6 | 92.9 | 98.3 | 99.4 | 96.5 |

The proposed formula has been tested against the collected numerical data. In particular, the section rigidity of the damaged section has been computed by using standard rules of the technical theory of beams. The obtained values are listed in table 4.

Table 4. Inertia moments of the various sections.

| Case | Layer 1 | | Layer 2 | | |
|---|---|---|---|---|---|
| | Height | Modulus | Height | Modulus | Inertia |
| | [m] | [MPa] | [m] | [MPa] | [m$^4$] |
| A | 0.80 | 6000 | - | - | 0.0427 |
| B | 0.70 | 6000 | 0.10 | 3000 | 0.0361 |
| C | 0.60 | 6000 | 0.20 | 3000 | 0.0320 |
| D | 0.65 | 6000 | 0.15 | 3000 | 0.0338 |
| E, G | 0.60 | 6000 | - | - | 0.0180 |
| F | 0.70 | 6000 | - | - | 0.0286 |

The damaged length of the various cases has been set to the whole arch length in the cases B, C, and D, while it resulted as 0.3, 0.8 and 1.2 in the remaining cases. The computation of the $k_D$ factors of formula (8) is straightforward.

The following Table 5 reports the comparison.

Table 5. Performance test of formula (8).

| Arch | Value | B [%] | C [%] | D [%] | E [%] | F [%] | G [%] |
|---|---|---|---|---|---|---|---|
| 180° | Average | 93.4 | 88.6 | 90.7 | 98.0 | 99.2 | 97.3 |
| 180° | Min | 90.9 | 84.9 | 87.6 | 93.4 | 96.8 | 91.3 |
| 180° | $k_D$ | 92.0 | 86.7 | 89.0 | 98.1 | 98.6 | 94.5 |
| 135° | Average | 93.9 | 89.3 | 91.6 | 97.7 | 99.1 | 100.6 |
| 135° | Min | 90.9 | 84.9 | 87.6 | 91.7 | 96.9 | 93.1 |
| 135° | $k_D$ | 92.0 | 86.7 | 89.0 | 97.5 | 98.2 | 98.5 |
| 90° | Average | 94.8 | 90.6 | 92.6 | 97.4 | 99.1 | 95.2 |
| 90° | Min | 91.0 | 84.9 | 87.7 | 88.8 | 94.6 | 93.5 |
| 90° | $k_D$ | 92.0 | 86.7 | 89.0 | 96.3 | 97.3 | 99.4 |
| | | | | | | | |
| 180° | error | 1.54 | 2.18 | 1.88 | -0.09 | 0.60 | 2.80 |
| 135° | error | 2.09 | 2.96 | 2.87 | 0.26 | 0.98 | 4.14 |
| 90° | error | 2.95 | 4.33 | 3.89 | 1.17 | 1.85 | 7.12 |

As is apparent in table 5, the errors involved in the simplified analysis are very small and allow a back calculation of the damage extent from the frequency shift recorded in an ambient vibration experiment.

As pointed out by Cruz and Salgado 2009, Tomor and Nichols 2015, Shallhorn 2012, the change in the frequency set is very different if we consider a distributed and a localized damage. In particular a generalised material decay is producing a proportional reduction on the whole frequency set, with a nearly linear relationship between the two parameters.

Generalized damages can arise as a consequence of fatigue, creep, or foundation settlements. Details on the techniques that allow detecting such rigidity changes can be gathered in Tomor and Verstrynge 2013, De Santis and Tomor 2015, Colla et Al. 1997.

In figure 4 the frequency shift due to homogeneous damage distributions B, C, and D, is presented. As is apparent, the average frequency shift is almost linear with the increase in thickness of the damaged layer.

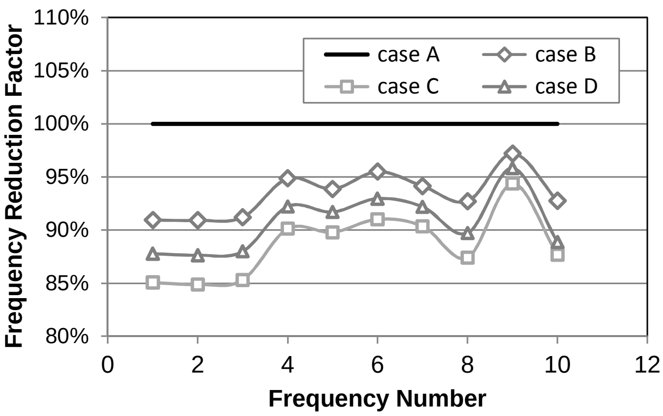


Fig. 4: Frequency shift of the 180° arch with continuous damage distributions.

On the other hand, the presence of a localized intake in the arches is producing an interleaving of the shifted frequency plots. Cruz and Salgado 2009, Tomor and Nichols 2015, and Brencich et Al. 2009, show that this behaviour is very common in real situations. Therefore this criterion, that means the standard deviation of the frequency shift, is very useful in pointing out the distribution of the damage.

The frequency shift of the examined cases E, F, and G for the 180° arch, are presented in figure 5.

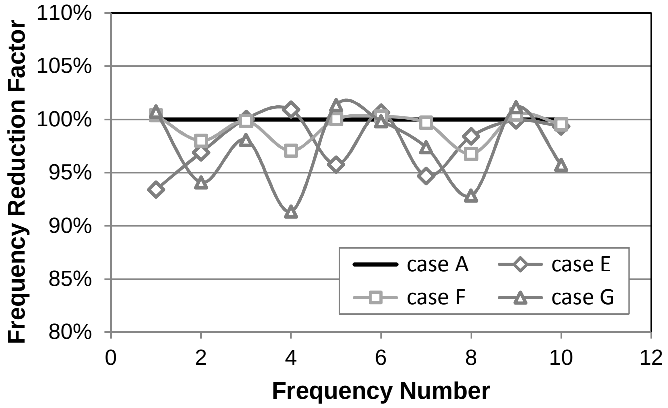


Fig. 5: Frequency shift for the examined cases of localized damage in the 180° arch.

The presented analysis of the damaged section is used to compute back the product $\rho \cdot \mu$ as a damage index from the average frequency decay of the computed frequency set. The computed values are compared with the exact damage indices gathered from the arch model geometries.

Table 6. Performance test of formula (13).

| Arch | Value | B | C | D | E | F | G |
|---|---|---|---|---|---|---|---|
| 180° | $n$ | 0.873 | 0.785 | 0.822 | 0.411 | 0.782 | 0.603 |
| 180° | $\rho \cdot \mu$ | 0.076 | 0.121 | 0.103 | 0.277 | 0.123 | 0.203 |
| 180° | exact | 0.063 | 0.125 | 0.094 | 0.250 | 0.125 | 0.250 |
| | error | 22% | -3% | 9% | 11% | -2% | -19% |
| 135° | $n$ | 0.882 | 0.798 | 0.839 | 0.449 | 0.813 | 0.641 |
| 135° | $\rho \cdot \mu$ | 0.071 | 0.115 | 0.094 | 0.263 | 0.107 | 0.187 |
| 135° | exact | 0.063 | 0.125 | 0.094 | 0.250 | 0.125 | 0.250 |
| | error | 13% | -8% | 0% | 5% | -14% | -25% |
| 90° | $n$ | 0.898 | 0.821 | 0.857 | 0.517 | 0.863 | 0.719 |
| 90° | $\rho \cdot \mu$ | 0.062 | 0.104 | 0.084 | 0.238 | 0.081 | 0.152 |
| 90° | exact | 0.063 | 0.125 | 0.094 | 0.250 | 0.125 | 0.250 |
| | error | -1% | -17% | -10% | -5% | -35% | -39% |

As is apparent in table 6, the errors involved in the reconstruction of the damage index is quite acceptable, assumed that the values are back calculated from the average frequency shift and not in function of the shift function. It seems however that the easiness of application of the proposed method could be a great improvement in the fast calculation of the efficiency status of existing bridges.

## 5 CONCLUSIONS

The paper presents some preliminary parametric analyses finalized at the statement of identification rules which can be preliminarily applied to real bridges in order to orient a computational procedure based on automated response acquisition at selected time intervals.

The problem of damage prediction based on natural frequency shift has had huge attention in the past and several review studies are available. However nowadays no definite procedure has emerged leading to a careful damage detection outside the laboratory environment.

Masonry bridges suffer of several types of progressive damage due to weathering, fatigue, creep, foundation settlement. Moreover, during a service life, masonry structures undergo a number of retrofitting operations and material strengthening.

As pointed out by Brencich & De Felice (2009), non-symmetric damages in masonry elements could produce a very large decay of resisting moment in eccentric compression.

Therefore the importance of defining a sensible and effective damage detection procedure is evident. The subdivision of the recorded signals with relation to a metric of different damage patterns is essential in order to direct the identification procedure toward the correct algorithm.

A very simple procedure for the estimation of the thickness of the damaged layer has been presented. The data needed for the calculation of the proposed damage index are, apart from the average frequency shift, the extension of the damaged zone in relation to the total length, and a fraction expressing the elastic modulus decay of the damaged zone.

The first preliminary assessment presented in this paper seems to point out that the simplified procedure highlighted in the paper can be sufficiently accurate in the damage estimation, although its computational effort is almost zero.

The need of wider laboratory assessments on scaled models is emerging clearly. These investigations can help in connecting data streams obtained by accelerometer recordings and real damage patterns assessed through static testing of the same artifacts.

## AKNOWLEDGMENTS

The present work is part of the SHAPE research project founded by the INFRAVATION program of the European Community. Rjikswaaterstaat as funding agency and European Community are kindly acknowledged.

## REFERENCES

Belluzzi O. 1960. *Scienza delle Costruzioni.* Vol. IV, Zanichelli Editore Bologna, Italy.

Benedetti A. Marani F. Ramalho M. 2010. Mechanical Properties of Masonry with Environmental Degradation. *Proceedings of the 8th International Masonry Conference*. Dresden, Germany July 4-7.

Brencich A. De Felice G. 2009. Brickwork under eccentric compression: Experimental results and macroscopic models. *Construction and Building Materials*. 23-5: 1935-1946.

Brencich A. Lagomarsino S. Riotto G. (2009). Dynamic Identification of reduced scale masonry bridges. *IOMAC'09*, Portonovo, Italy.

Colla C. Das P.C. McCann D. Forde M.C. 1997. Sonic, electromagnetic and impulse radar investigation of stone masonry bridges. *NDT & E International*. 30-4: 249-254.

Cruz P. Salgado R. 2009. Performance of Vibration-Based Damage Detection Methods in Bridges. *Computer-Aided Civil and Infrastructure*. 24(1):62-79.

De Santis S. Tomor A. 2013. Laboratory and field studies on the use of acoustic emission for masonry bridges. *NDT & E International*, 55(4): 64-74.

Doebling S.W Farrar C.R. Prime M.B. Shevitz D.W. 1996. *Damage Identification and Health Monitoring of Structural and Mechanical Systems from Changes in Their Vibration Characteristics: A Literature Review*. LA-13070-MS, Los Alamos Nat. Lab. New Mexico 87545 USA.

Gillich G.R. Praisach Z.I. 2014. Modal identification and damage detection in beam-like structures using the power spectrum and time–frequency analysis. *Signal Processing* 96:29-44.

Öz H.R., Daş M.T. 2006. In-plane vibrations of circular curved beams with a transverse open crack. *Mathematical and Computational Applications*. 11-1: 1-10.

Pelà L. Aprile A. Benedetti A. 2009. Seismic Assessment Of Masonry Arch Bridges. *Engineering Structures*. 31-8: 1777-1788.

Salawu O. S. 1997. Detection of structural damage through changes in frequency: a review. *Engineering Structures* 19(9): 718-723.

Shallhorn C.J. 2012. Localization of vibration-based damage detection method in structural applications. MS thesis, University of Iowa, http://ir.uiowa.edu/etd/3529.

Tomor A. and Nichols J. M. 2015. Monitoring changes in natural frequency and deterioration for masonry arch bridges with Fast Fourier transform. *Proc. of 12th North American Masonry Conference*. Denver, Colorado May 17 – 20.

Tomor A. Verstrynge E. 2013. A joint fatigue–creep deterioration model for masonry with acoustic emission based damage assessment. *Construction and Building Materials.* 43(6): 575-588.